

# Analysing the Effect of the Vehicle's Length on the Aerodynamic Drag

Ahmed A. S. Al-Saadi<sup>1</sup>, Kadhim Al-Chlahawi<sup>1</sup>, Ammar Abdulkadhim<sup>2</sup>

<sup>1</sup>Department of mechanical engineering, College of engineering, University of Al-Qadisiyah, Al-Qadisiyah, Iraq

<sup>2</sup> Air conditioning and Refrigeration Techniques Engineering Department, Al-Mustaqbal University College, Babylon, Iraq

**Abstract.** In overall car performance and ride stability, external car aerodynamic study is of great importance, making it a key element in effective automobile design. In this study, the effect of the vehicle's length on the drag coefficient was numerically investigated. For this purpose, a CFD analysis based on RANS turbulence models was carried out for six configurations for the Ahmed body model with different length in addition to the baseline model. Tetrahedral cells were adopted throughout air enclosure except some prism cells around the vehicle's surfaces. Good agreement for the benchmark model was obtained by comparing current numerical results with experimental related data. The numerical results demonstrate that 1244mm is the optimal length of the Ahmed body. Increasing the overall length of the Ahmed body by about 19.15% leads to decreasing drag coefficient by 8.95%.

**Keywords:** Aerodynamics; Turbulent flow; Ahmed body; CFD; RANS; Drag coefficient; Vehicle's length; fuel consumption.

## Introduction

Aerodynamics is simply focusing on the fluid flows over bodies like airfoils, cars, missiles, rocket etc. Numerous researchers studied this science due to its contribution in industrial applications. The researchers tries to reduce the drag force as it considered as one of the main barriers to accelerate road vehicles, just to overcome this adverse aerodynamic force, about 50 to 60 percent of total burned fuel energy get lost [1]. Due to the legislations of the environmental protection agency to minimize the harmful emissions as well as consumer requirements for fuel economy vehicles, the aerodynamic drag reduction has been a very significant issue for the automakers over the last two decades [2]. In the automotive industry, the aerodynamic ability as well as the car model's appearance are the deciding factors in attracting the interest of customers. The car body design is the most complex and important part in the field of automotive production, where there are number of constraints make it a challenging one such as space, esthetics, appeal, style and aerodynamically refined [3, 4]. Therefore, and from the early days, the designers understood the significance of drag coefficient reduction and a lot of studies were carried out in this field [5-7]. Various researchers used different numerical approaches using CFD for treating the turbulent flows in aerodynamics problems especially large-eddy simulation [8-10], direct numerical simulation [11] along with RANS simulation [12]. Song et al. [13] obtained a 5.6% reduction in  $C_D$  of the sedan car by modifying the rear body shapes. Al-Saadi, et al. [14] showed that, via three dimensional CFD simulation, the aerodynamic drag coefficient of Land Rover Discovery model reduced by 9.53%. Cho et al. [15] found that the sedan-type car with undercover can reduce the vehicle aerodynamic drag by 8.4 percent. Tian, et al. [16] numerically showed that the edges slant surfaces of a standard Ahmed model with flap structures reduced the values of drag by about 21.1%, 21.2% and 17.9% for the configuration angles of 80°, 40° and 20° respectively.

Shankar and Devaradjane [17] observed that the car drag and lift coefficients reduced by 4.53% and 2.55% respectively by vortex generators with leading edges toward back end and the middle plane of the vehicle. Shadmani, et al. [18] experimentally demonstrated that drag force of Ahmed body with plasma actuator system situated in the center of the rear slant surface can be decreased by 3.65% and 2.44% in steady and un steady actuations respectively. Additionally, the impact of ground clearance had been studied a lot as in [19-26]

The impact of car modification on reducing the drag had been investigated a lot in terms of changing the shape of the geometries utilizing different turbulence model. The baseline model in this study is Ahmed body, as the most famous geometry in aerodynamic of road vehicles. For example, a comparison study between different turbulence models in order to investigate the models that reveals better solution had been examined by [27] that had been applied on Ahmed body model. PIV techniques had been implemented also by [28] in order to visualize the fluid flow over a bus model. There are studies focusing on the study of the wake region as it affect the drag. For example, [29] deduced experimentally as well as numerically that vortex generator reduces the wake region which attains the augmentation of car efficiency. [30] used k-epsilon turbulent model to study the near-wake of Ahmed body considering RANS equations to examine the influence of slack angle of Ahmed model. [31] LES had been used also to investigate the slant angle on drag [32] studied the impact of windshield using CFD code on drag reduction and fuel consumption. [33] utilized CATIA program to design a bus and simulated numerically utilizing ANSYS FLUENT in order to examine the influence of bus shape under velocities of (80-120) kmph on drag force. [34] investigate the impact of adding devices on the back of the model which was square model in order to reduce the drag.

It can be seen based upon the mentioned comprehensive review on the Ahmed model that the angle of slant had been studied a lot under different wind velocities and turbulence models but there are serious limitations regarding the influence of length of Ahmed model on drag coefficient. Thus, in addition to this work is aimed to study the effect of the vehicle's length on the drag coefficient and to investigate the optimum length of car. Computational approach is applied to identify the optimum length. CFD simulations were performed with ANSYS Fluent 16.0 software. Six modified length models, in addition to the standard model are investigated in order to study the effect of overall length of vehicle on the drag coefficient.

### Numerical Simulation

All computational models in this study, baseline and modified models, are created by using SolidWorks while the CFD simulations are accomplished using ANSYS Fluent.

The motion of any fluid flow can be explained via the governing equations. Conservation equations of momentum, mass and energy represent governing equations in the present study which is known as Navier Stokes equations. Most numerical studies of fluid flow around the bluff body are based principally on RANS equations [35]. Realizable  $k-\varepsilon$  turbulence model has a wall function technique to correct the numerical results near the surfaces of the vehicle. Therefore, no need to use high quality mesh near surfaces. On the other hand,  $k-\varepsilon$  is suitable for high Reynolds number. Other turbulence models (SST and LES) are computationally expensive. The realizable  $k-\varepsilon$  model was applied in all simulations.

Transport equations for  $k$  and  $\varepsilon$  were as following [36], [37]:

$$\frac{\partial(\rho k)}{\partial t} + \text{div}(\rho k \mathbf{U}) = \text{div}\left[\left(\frac{\mu_t}{\sigma_k}\right) \text{grad}(k)\right] + 2\mu_t S_{ij} \cdot S_{ij} - \rho \varepsilon \quad (1)$$

$$\frac{\partial(\rho \varepsilon)}{\partial t} + \text{div}(\rho \varepsilon \mathbf{U}) = \text{div}\left[\left(\frac{\mu_t}{\sigma_\varepsilon}\right) \text{grad}(\varepsilon)\right] + C_{1\varepsilon} \left(\frac{\varepsilon}{k}\right) 2\mu_t S_{ij} \cdot S_{ij} - C_{2\varepsilon} \rho \left(\frac{\varepsilon^2}{k}\right) \quad (2)$$

The eddy viscosity is [36]:

$$\mu_t = \rho C_\mu \frac{k^2}{\varepsilon} \quad (3)$$

The drag coefficient ( $C_D$ ) is calculated based on the following equation [38]:

$$C_D = \frac{2 F_D}{(\rho V^2 A)} \quad (4)$$

While the following equation is used to calculate the lift coefficient ( $C_L$ ) [38]:

$$C_L = \frac{2 F_L}{(\rho V^2 A)} \quad (5)$$

Ahmed body was used as a simplified car model for aerodynamic analysis in this study. The Ahmed body has a rear slant angle of 25°. Its body length of 1044mm while it's body height of 338mm. In addition to the Ahmed's body width of 389mm. Fig. 1 illustrates the standard Ahmed body with dimensions. Six modified lengths (844, 944, 1144, 1244, 1344 and 1444mm), in addition to the standard model were investigated to study the effect of the vehicle's length on the aerodynamic performance. Two different models have overall less length than baseline model (configurations 1 and 2). While four different modified Ahmed body models have more length than standard model (configurations 4, 5, 6 and 7). In addition to the baseline model which represented in configuration 3 as shown in Table 1.

Table 1. Seven different configurations of the Ahmed body.

Configuration	H (height)	L (length)	H/L
1	338	844	0.4
2	338	944	0.358
3	338	1044	0.324
4	338	1144	0.295
5	338	1244	0.272
6	338	1344	0.251
7	338	1444	0.234

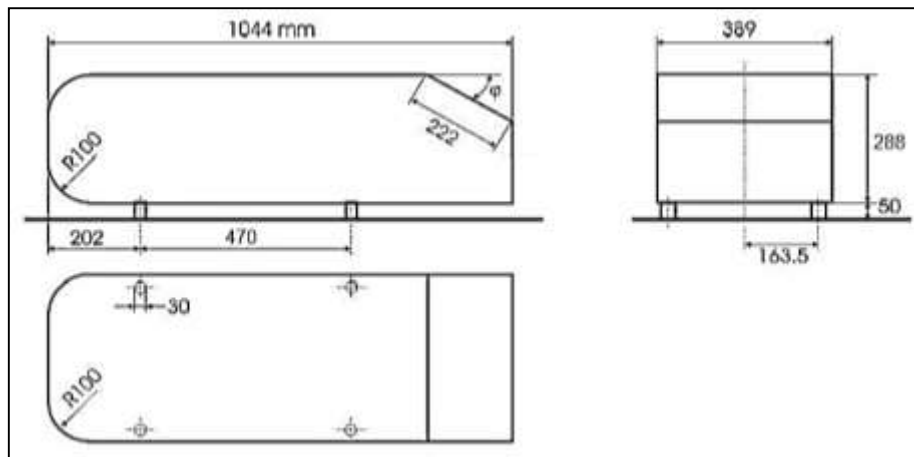


Figure 1. Standard Ahmed body [39].

SolidWorks software was used to create all computational vehicle models in this study. The computational domain was formed using ANSYS Fluent software. It consists of inlet, outlet, side walls, top wall (roof), bottom wall (road). Fig. 2 represents the computational domain used in all simulations.

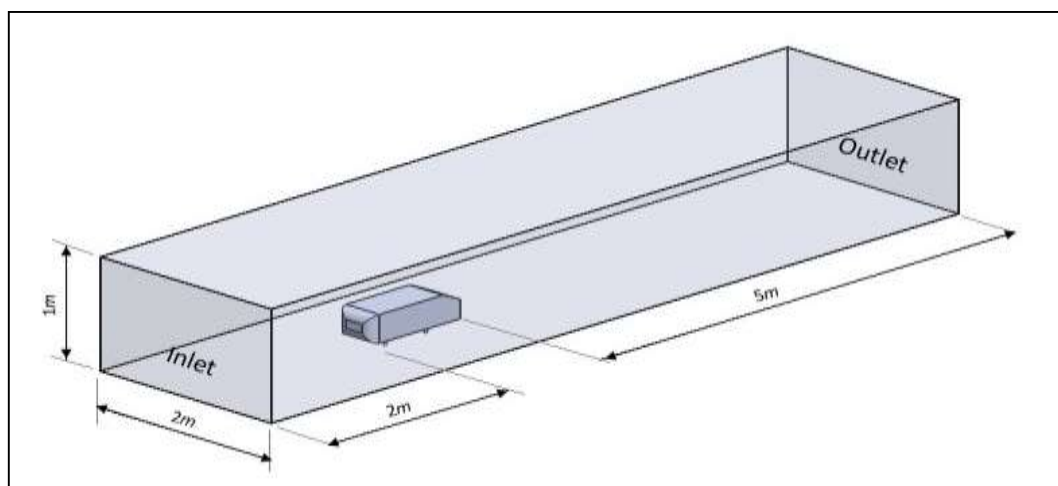


Figure 2. Numerical computational domain.

The tetrahedral cells throughout computational domain and prism cells around Ahmed's surfaces were generated using ANSYS meshing. Five prismatic layers were used around all surfaces of the Ahmed body as well as over the road to increase the accuracy of results. Mesh refinement with varying levels was adopted to obtain high quality mesh. A range between  $250 \times 10^3$  and  $15 \times 10^6$  was used for the total number of cells to achieve the optimal number of cells as mentioned in the next section (computational results). Three volumetric control boxes around the vehicle model are included within the refinement to control growth ratio which was 1.2. The mesh inside computational domain for the Ahmed body model is presented in Fig. 3.

Boundary conditions used in all numerical simulations were similar to those adopted in the experimental tests. Uniform initial air velocity was used between 6.8 m/s and 77 m/s. Stationary surfaces of vehicle with no slip were adopted. All computational domain walls were stationary with no slip as in the experimental tests.

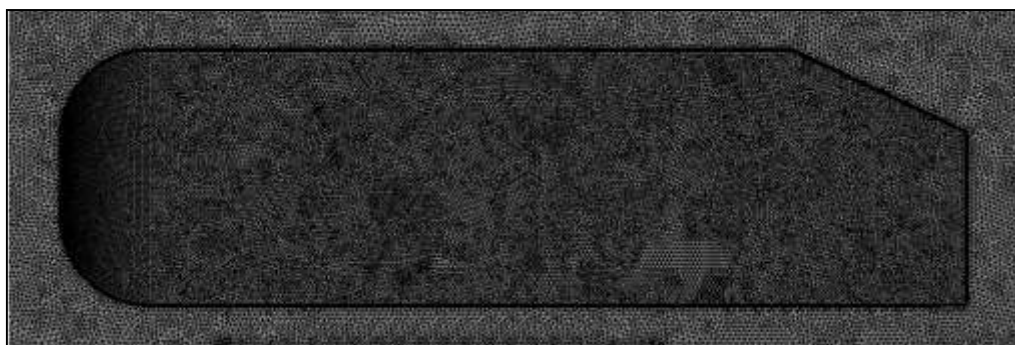


Figure 3. Mesh of the standard model of the Ahmed body (Side view).

## Computational results

The simulation results of all configurations, standard Ahmed body and all modified models, are described in this section. Grid independence for the benchmark was investigated for a wide range of mesh density. It is found that  $5.8 \times 10^6$  cells for half computational domain is the optimal number of cells as shown in Fig. 4.

Comparing the simulation results of standard Ahmed body with some experimental data was achieved first in order to validate the numerical method which was used in this study. The numerical results of the current study have a similar overall behaviour to the particular studies of Ahmed et al. [39], Meile et al. [40] and Bello-Millán et al. [41] as shown in Fig. 5. The percentage error between present numerical study and other previous studies were between 2% (Ahmed et al.) and 20% (Thacker et al.). Table 2 illustrates all percentage error between current study and related studies.

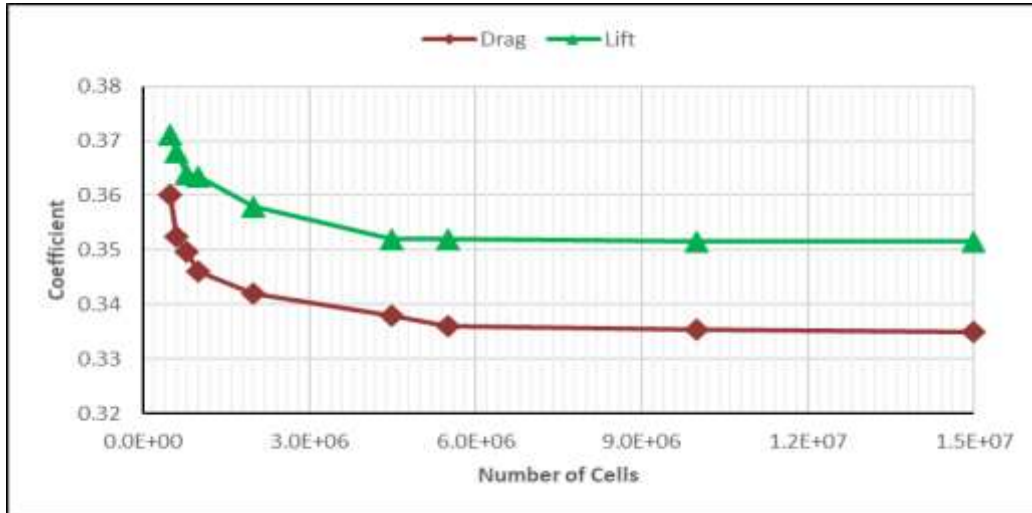


Figure 4. Lift and drag coefficients as a function to number of cells.

Seven different configurations of the Ahmed body (as described in Table 1) were simulated in order to achieve the optimal length for this bluff body. Pressure drag and skin friction drag are the two components of the total drag coefficient.

The faster regions of the flow within boundary layer are affected by the slower regions. Therefore, internal shear stresses increase in boundary layer due to the velocity gradient. This friction is known as skin-friction drag. Flow over curved surfaces lead to increase the pressure in the flow direction. Resulting in an unstable boundary layer and separating the flow from the car surfaces. This kind of drag is called pressure drag.

Fig. 6 shows total drag and its components. Skin friction drag depends on the total surfaces of the vehicle. Therefore, long vehicles have higher drag of skin friction than short vehicles as shown in Fig. 6 (green curve). While the long vehicle has pressure drag less than short vehicle as shown in Fig. 6 (red curve). The minimum total drag is at 0.27 of H/L. The optimal length of the Ahmed body is 1244mm.

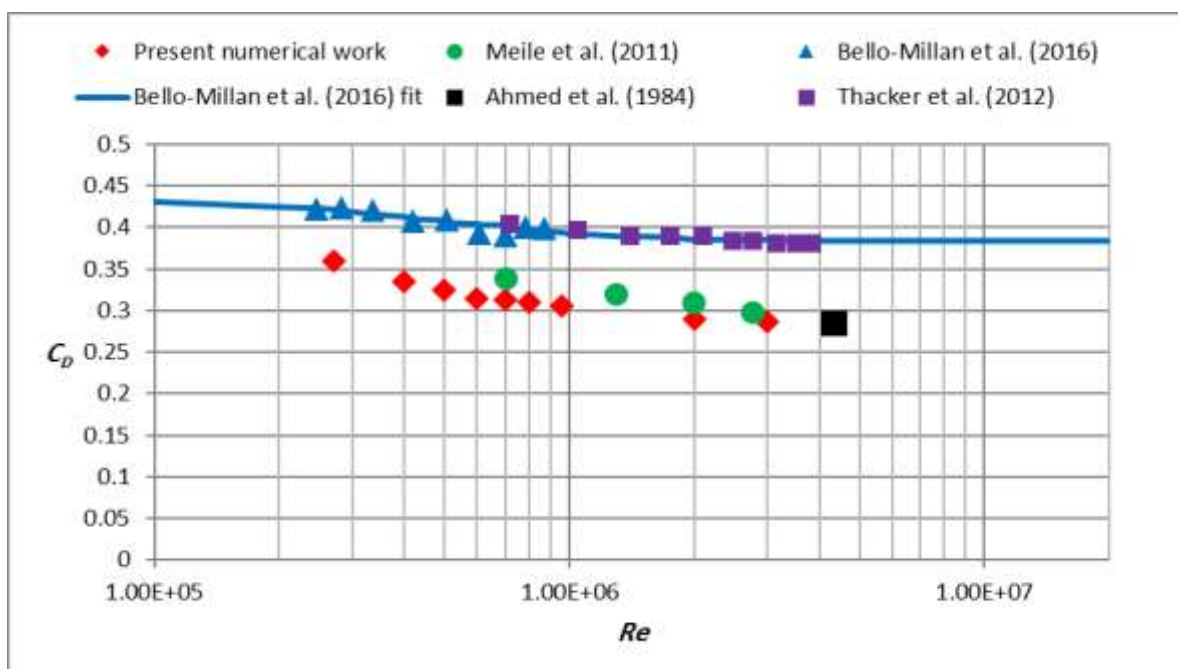


Figure 5. Comparative between current study and relative studies for standard Ahmed body.

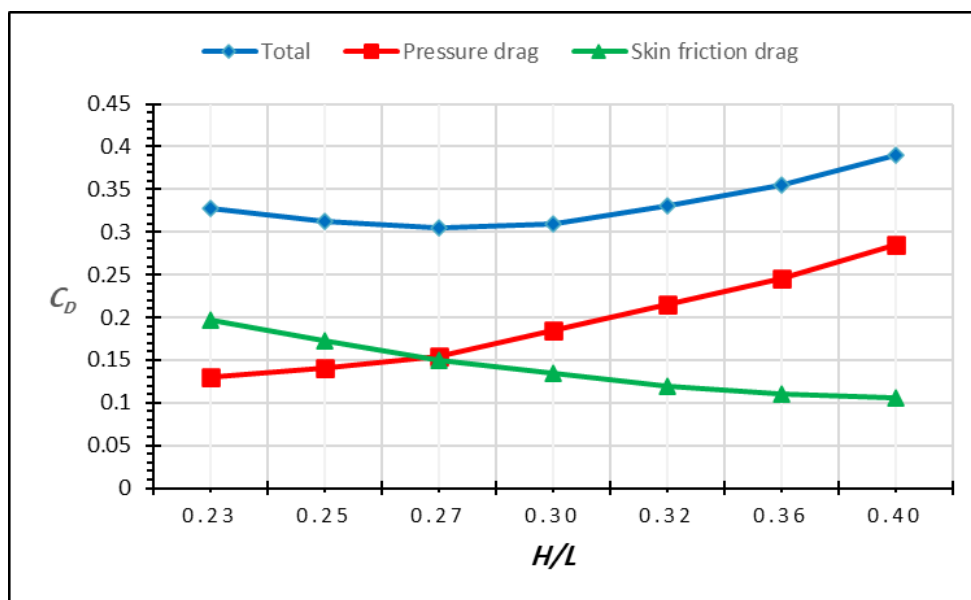


Figure 6. Pressure drag, skin friction drag and total drag for all configurations of the Ahmed body model (6 modified models and standard model).

Table 2. Percentage error between current study and related studies.

	<i>Bello-Millan et al. (2016)</i>	<i>Meile et al. (2011)</i>	<i>Thacker et al. (2012)</i>	<i>Ahmed et al. (1984)</i>
Percentage error (%)	14	6	20	2

## Conclusions

Mesh density has a great influence on the drag and lift coefficients. Therefore, testing mesh independency is a crucial step in numerical simulation. All numerical  $C_D$  of the Ahmed body are in agreement with previous related experimental data for a wide range of  $Re$ . Standard Ahmed body and six configurations of the Ahmed body model with different length were investigated in order to achieve minimum drag coefficient. Increasing surface area of vehicle leads to increase in drag of skin friction. Pressure drag increases with decreasing of vehicle length.

Separation of boundary layer occurs faster in short vehicle than long one. Therefore, pressure drag for the short length vehicle is higher than long vehicle for the same design. While the skin friction is vies versa.

The optimal length of vehicle is at the intersection drag of skin friction with pressure drag. Increasing the overall length of the Ahmed body by about 19.15% leads to decreasing drag coefficient by 8.95%. Air resistance forms about 50% of the overall moving resistance when the vehicle moves at 27.77m/s. Therefore, half engine power of the vehicle is consumed by the aerodynamic drag while the rest is dissipated by rolling resistance. Reducing drag by 9% in optimal length leads to 4.5% reduction in fuel consumption.

## References

- Hassan, S.R., et al., *Numerical study on aerodynamic drag reduction of racing cars*. Procedia Engineering, 2014. **90**: p. 308-313.
- Zhang, C., et al., *Full vehicle CFD investigations on the influence of front-end configuration on radiator performance and cooling drag*. Applied Thermal Engineering, 2018. **130**: p. 1328-1340.
- Gunpinar, E., et al., *A generative design and drag coefficient prediction system for sedan car side silhouettes based on computational fluid dynamics*. Computer-Aided Design, 2019. **111**: p. 65-79.
- Paul, A.R., A. Jain, and F. Alam, *Drag reduction of a passenger car using flow control techniques*. International Journal of Automotive Technology, 2019. **20**(2): p. 397-410.
- Sudin, M.N., et al., *Review of research on vehicles aerodynamic drag reduction methods*. International Journal of Mechanical and Mechatronics Engineering, 2014. **14**(02): p. 37-47.
- Singh, J. and J.S. Randhawa, *CFD analysis of aerodynamic drag reduction of automobile car-a review*. International Journal of Science and Research, 2014. **3**(6): p. 213-215.
- Mukut, A.M.I. and M.Z. Abedin, *Review on Aerodynamic Drag Reduction of Vehicles*. International Journal of Engineering Materials and Manufacture, 2019. **4**(1): p. 1-14.
- Spalart, P.R. *Comments on the feasibility of LES for wings, and on a hybrid RANS/LES approach*. in *Proceedings of first AFOSR international conference on DNS/LES*. 1997. Greyden Press.
- Temmerman, L., et al., *Investigation of subgrid-scale models and wall-functions approximations in large eddy simulation of separated flow in a streamwise periodic channel constriction*. Int. J. Heat Fluid Flow, 2003. **24**: p. 157-180.

10. Jansson, N., J. Hoffman, and M. Nazarov. *Adaptive simulation of turbulent flow past a full car model*. in *SC'11: Proceedings of 2011 International Conference for High Performance Computing, Networking, Storage and Analysis*. 2011. IEEE.
11. Ishida, T., P. Davidson, and Y. Kaneda, *On the decay of isotropic turbulence*. *Journal of Fluid Mechanics*, 2006. **564**: p. 455-475.
12. Pope, S.B. and S.B. Pope, *Turbulent flows*. 2000: Cambridge university press.
13. Song, K.-S., et al., *Aerodynamic design optimization of rear body shapes of a sedan for drag reduction*. *International Journal of Automotive Technology*, 2012. **13**(6): p. 905-914.
14. Al-Saadi, A., A. Hassanpour, and T. Mahmud, *Simulations of Aerodynamic Behaviour of a Super Utility Vehicle Using Computational Fluid Dynamics*. *Adv Automob Eng*, 2016. **5**(134): p. 2.
15. Cho, J., et al., *Comparative investigation on the aerodynamic effects of combined use of underbody drag reduction devices applied to real sedan*. *International Journal of Automotive Technology*, 2017. **18**(6): p. 959-971.
16. Tian, J., et al., *Aerodynamic drag reduction and flow control of Ahmed body with flaps*. *Advances in Mechanical Engineering*, 2017. **9**(7): p. 1687814017711390.
17. Shankar, G. and G. Devaradjane, *Experimental and computational analysis on aerodynamic behavior of a car model with vortex generators at different yaw angles*. *Journal of Applied Fluid Mechanics*, 2018. **11**(1): p. 285-295.
18. Shadmani, S., et al., *Experimental study of flow control over an Ahmed body using plasma actuator*. *Mechanics and Mechanical Engineering*, 2020. **22**(1): p. 239-252.
19. Anderson, H., *Investigation of the forces on bluff bodies near the ground*. 1977, M. Sc. thesis, Department of Aeronautics, Imperial College.
20. Bearman, P., *Bluff body flows applicable to vehicle aerodynamics*. 1980.
21. George, A., *Aerodynamic effects of shape, camber, pitch, and ground proximity on idealized ground-vehicle bodies*. 1981.
22. Garry, K.P., *Some effects of ground clearance and ground plane boundary layer thickness on the mean base pressure of a bluff vehicle type body*. *Journal of wind engineering and industrial aerodynamics*, 1996. **62**(1): p. 1-10.
23. Zhang, X., A. Senior, and A. Ruhrmann, *Vortices behind a bluff body with an upswept aft section in ground effect*. *International Journal of Heat and Fluid Flow*, 2004. **25**(1): p. 1-9.
24. Zhang, X., W. Toet, and J. Zerihan, *Ground effect aerodynamics of race cars*. 2006.
25. Dong, T., et al., *The effect of reducing the underbody clearance on the aerodynamics of a high-speed train*. *Journal of Wind Engineering and Industrial Aerodynamics*, 2020. **204**: p. 104249.
26. Quazi, A., et al., *A field study on the aerodynamics of freight trains*. *Journal of Wind Engineering and Industrial Aerodynamics*, 2021. **209**: p. 104463.
27. Guilmineau, E., G. Deng, and J. Wackers, *Numerical simulation with a DES approach for automotive flows*. *Journal of Fluids and Structures*, 2011. **27**(5-6): p. 807-816.
28. Gurlek, C., B. Sahin, and G.M. Ozkan, *PIV studies around a bus model*. *Experimental Thermal and Fluid Science*, 2012. **38**: p. 115-126.
29. Gopal, P. and T. Senthilkumar, *Influence of Wake Characteristics of a Representative Car Model by Delaying Boundary Layer Separation*. *Journal of Applied Science and Engineering*, 2013. **16**(4): p. 363-374.
30. Tientcheu-Nsiewe, M., et al., *Numerical Study of a Turbulent Flow in the Near-Wake of an Ahmed Body*. *American Journal of Environmental Engineering*, 2016. **6**(6): p. 157-163.
31. Franck, G., et al., *Numerical simulation of the flow around the Ahmed vehicle model*. *Latin American applied research*, 2009. **39**(4): p. 295-306.
32. BAYINDIRLI, C. and M. Çelik, *The determination of effect of windshield inclination angle on drag coefficient of a bus model by CFD method*. *International Journal of Automotive Engineering and Technologies*. **9**(3): p. 122-129.
33. Jadhav, C.R. and R.P. Chorage, *Modification in commercial bus model to overcome aerodynamic drag effect by using CFD analysis*. *Results in Engineering*, 2020. **6**: p. 100091.
34. Khalighi, B., K.-H. Chen, and G. Iaccarino, *Unsteady aerodynamic flow investigation around a simplified square-back road vehicle with drag reduction devices*. *Journal of fluids engineering*, 2012. **134**(6).
35. Zaki, M., S. Menon, and L.N. Sankar, *Hybrid Reynolds-Average Navier-Stokes and Kinetic Eddy Simulation of External and Internal Flows*. *Journal of aircraft*, 2010. **47**(3): p. 805-811.
36. Versteeg, H.K. and W. Malalasekera, *An introduction to computational fluid dynamics: the finite volume method*. 2007: Pearson education.
37. Iqbal Qureshi, M.Z. and A.L.S. Chan, *Influence of eddy viscosity parameterisation on the characteristics of turbulence and wind flow: Assessment of steady RANS turbulence model*. *Journal of Building Engineering*, 2020. **27**: p. 100934.
38. Schuetz, T., *Aerodynamics of road vehicles*. 2016: SAE.

39. Ahmed, S.R., G. Ramm, and G. Faltin, *Some salient features of the time-averaged ground vehicle wake*. SAE Transactions, 1984: p. 473-503.
40. Meile, W., et al., *Experiments and numerical simulations on the aerodynamics of the Ahmed body*. CFD letters, 2011. **3**(1): p. 32-39.
41. Bello-Millan, F., et al., *Experimental study on Ahmed's body drag coefficient for different yaw angles*. Journal of Wind Engineering and Industrial Aerodynamics, 2016. **157**: p. 140-144.